ACS OMEGA

http://pubs.acs.org/journal/acsodf

Article

Advanced Optical Characterization of PEDOT:PSS by Combining Spectroscopic Ellipsometry and Raman Scattering

Minghua Kong, Miquel Garriga, Juan Sebastián Reparaz, and Maria Isabel Alonso*

Cite This: *ACS Omega* 2022, 7, 39429−39436

Read Online

ACCESS | Metrics & More | Article Recommendations | Supporting Information

ABSTRACT: The optical properties of various PEDOT:PSS films obtained by drop casting and blade coating are analyzed by variable-angle spectroscopic ellipsometry in the visible-UV spectral range. We discuss observed differences in the optical spectra due to PSS content and DMSO treatment and correlate them to structural changes extracted from Raman measurements. In particular, we investigate the optical anisotropy of the complex refractive indices which arises from the in-plane arrangement of the PEDOT backbones, giving rise to optically uniaxial behavior with the optic axis perpendicular to the film plane. Although this is widely accepted, most investigations disregard the anisotropy for simplicity, which sometimes leads to inaccurate conclusions. In this work, we compare the results of isotropic and anisotropic analyses to clarify which kind of errors we can expect if anisotropy is not considered. Finally, the correlation between Raman scattering and ellipsometric analyses shows that not only local structural changes of the chain conformation but also the overall morphology of the composite films are significant in the interpretation of Raman spectra.

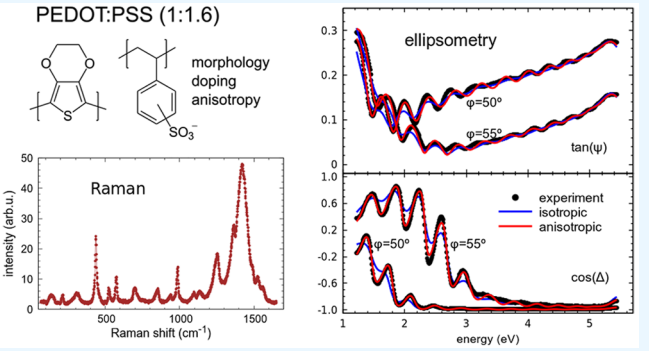

1. INTRODUCTION

Poly(3,4-ethylenedioxythiophene):poly(styrenesulfonate) (PEDOT:PSS) is a widely used organic material in many fields of application,[1] particularly in optoelectronic devices, as a flexible electrode for solution-processed solar cells and light-emitting diodes, acting as hole transport and hole injection layer, respectively.[2] Understanding the optical properties of these films to model the optical behavior of such devices is important for their proper design and optimization.

It is widely accepted that PEDOT:PSS thin films are optically anisotropic, displaying uniaxial behavior with the optic axis perpendicular to the film plane. Other PEDOT composites have similar optical anisotropy, since it originates in the in-plane arrangement of the PEDOT backbones that results from most solution processes. The anisotropy is also influenced by the composite nature of the films in which PEDOT:PSS grains are surrounded by excess nonconductive PSS. Therefore, the final structure and properties of the films mainly depend on the PSS content of the specific formulation, but also on other film treatments, like DMSO addition, that modify the morphology.[1,2] This structural variability is reflected in the anisotropic complex refractive indices of the films which are usually determined by spectroscopic ellipsometry. However, most investigations disregard the anisotropy and assume that PEDOT:PSS films are optically isotropic for simplicity.[4,5] This assumption may be approximately valid sometimes but not always, and in fact it may lead to erroneous conclusions when optical simulation of the devices is needed.[6] In addition, even if not many authors have published reference values of anisotropic complex refractive indices of PEDOT:PSS, considerable scatter of data is found in the literature, which is also partly due to the use of isotropic approximations without clear comparison between isotropic and anisotropic analyses evidencing which kind of errors can be expected when anisotropy is not considered. The two components of the uniaxial complex refractive index of PEDOT:PSS in a wide spectral range were reported in the seminal work of Pettersson et al.[3] for spin-coated films of the Baytron P formulation (1:1.25 ratio by weight). Other reported values are those of Heraeus Clevios PH500[7] and PH1000,[8,9] both containing a 1:2.5 weight ratio. Finally, spin-coated films of Heraeus Clevios AI4083 (1:6) were reported to be optically almost isotropic,[10] although their electrical conductivity was found to be clearly anisotropic.[11] A systematic optical investigation of different formulations including anisotropy and structural considerations is not found at hand.

Received: September 13, 2022
Accepted: October 6, 2022
Published: October 18, 2022

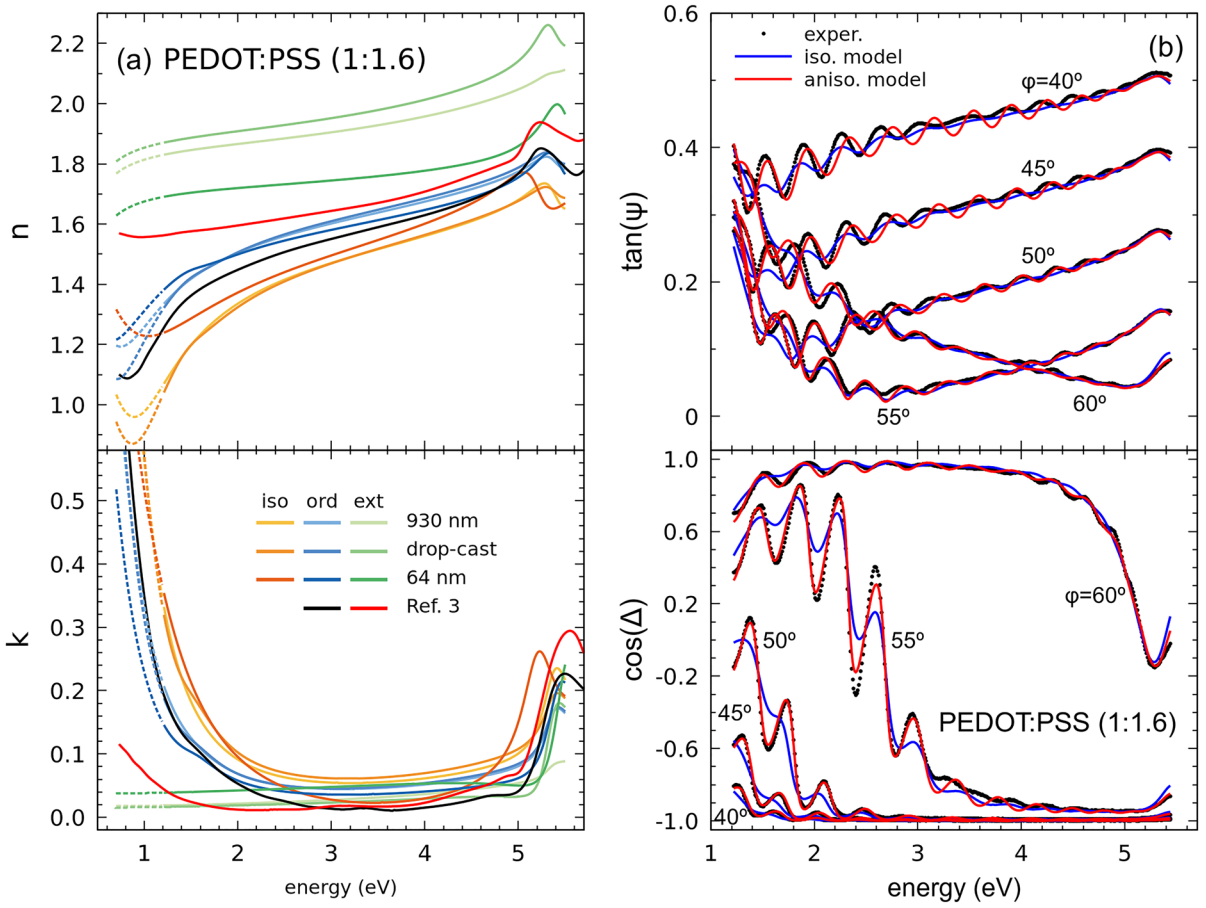

Figure 1. (a) Complex refractive index components for different films of Sigma-Aldrich 483095 PEDOT:PSS. Data extracted from ref 3 are plotted for comparison. (b) Experimental spectra and fits using both isotropic and anisotropic models for the thinner (d = 930 nm) dropcast film.

In this work, we set to rationalize changes in anisotropic complex refractive indices observed in different PEDOT:PSS films. We discuss the anisotropic optical behavior of two quite different commercial PEDOT:PSS formulations, namely, Sigma-Aldrich 483095 (1:1.6 ratio by weight) and Heraeus Clevios AI4083 (1:6), compared with values found in the literature. We also compare these results to isotropic approximations and examine the ellipsometric analysis for very different film thicknesses, from rather thick drop cast samples to thinner films obtained by blade coating, similar to those used in actual devices. We also study dimethyl sulfoxide (DMSO) treated material and correlate the observed variations to structural changes that can be identified from Raman measurements.

2. EXPERIMENTAL SECTION

2.1. Samples. We investigated a large number of samples from which we selected a few representative ones illustrating the typical behaviors observed in general. The films were deposited by blade-coating or drop casting as detailed in the Supporting Information. In particular, we needed to compare a large span of thicknesses from very thin (blade-coating) to very thick (drop casting) to demonstrate that the values of anisotropic optical functions we obtain from our fits are reliable. Different qualitative aspects of the measured spectra are more evident in films of different thicknesses, which helps to establish the appropriate data analysis.

For the Sigma-Aldrich 483095 formulation, we selected two pristine drop cast films, a thick one (>3 μm) and a thinner one of 930 nm, a pristine blade-coated film of 64 nm thickness, and a thick drop cast dried from a 50% H_2O:DMSO solution.[12] For the Heraeus Clevios AI4083 formulation we selected a thick drop cast film, two blade-coated films of similar thicknesses (87 and 62 nm thick) fabricated in different batches, and a thick drop cast also modified with 50% v/v DMSO.

2.2. Optical Spectroscopic Methodologies. *2.2.1. Ellipsometry Data Fitting.* In what follows, we describe in detail, as an illustrative example, the analysis of ellipsometry data for the more conductive studied formulation of PEDOT:PSS, namely, Sigma-Aldrich 483095, which displays stronger optical anisotropy. We fit the measured ellipsometric magnitudes tan ψ and cos Δ using both an isotropic model and an uniaxial anisotropic model in which the optic axis of the film is perpendicular to its surface and compare both results. Since all films have low roughness, for the analysis, we just consider one film on the isotropic glass substrate, which was separately measured and fitted as reference.

The complex dielectric function of PEDOT:PSS can be parametrized using well-known analytic line shapes.[13] The metallic-like behavior given by the bipolaron band[2] is described using the Drude model, whereas other observed contributions such as the polaron band or interband transitions are added as generalized Lorentzians, e.g., zero-dimensional critical points (CPs). Hence, the general line shape used is

https://doi.org/10.1021/acsomega.2c05945
ACS Omega 2022, 7, 39429−39436

$$\varepsilon(E) = \varepsilon_\infty - \frac{{E_p}^2}{E^2 + iE\Gamma_p} + \sum_j \frac{A_j e^{i\varphi_j}}{E - E_j + i\Gamma_j} \quad (1)$$

where E_p corresponds to the unscreened plasma energy of the free carriers and Γ_p gives their scattering rate. The screened energy of the free-carrier plasma oscillations is given by $E_p/\sqrt{\varepsilon_\infty}$, where the constant term ε_∞ is real. The parameters of each CP are the amplitude A_j, the phase ϕ_j, the transition energy E_j and the broadening Γ_j. The Drude model parameters can be related to the electrical resistivity according to

$$\rho\ (\Omega\ \mathrm{cm}) = \frac{4\pi\hbar}{\varepsilon_0}\frac{\Gamma_p}{\varepsilon_\infty E_p^2} = 0.58695\frac{\Gamma_p}{\varepsilon_\infty E_p^2} \quad (2)$$

The constant factor is calculated so that units of ρ in eq 2 are Ω cm when both Γ_p and E_p are inserted in eV. The values of electrical resistivity calculated in this way are helpful to establish relative comparison between films and to provide estimated values which are often smaller than the dc resistivity obtained from electrical measurements. One reason for this discrepancy is the simplistic model but also the higher sensitivity of the electrical measurement to the presence of macroscopic defects in the film.[14] The Drude parameters are also useful to estimate the carrier mobility μ and concentration N_p which are given by $\mu\ (\mathrm{cm}^2/(\mathrm{V\ s})) = 7.2739/\Gamma_p m^*$ and $N_p\ (\mathrm{cm}^{-3}) = 7.2525 \times 10^{20} \cdot E_p^2 \varepsilon_\infty m^*$, respectively, where m^* is the effective mass of the charge carriers and both Γ_p and E_p are expressed in eV. These approximations are mainly useful to establish relative comparisons among samples. For that, the effective mass can be taken as 1 or use theoretical values calculated using density functional theory (DFT) methods.[15] Notice that m^* is anisotropic, for example, in a pristine crystal, the effective mass for the holes is 0.13 along the backbone or 4.8 in the π-stacking direction, and these values do not change much in a heavily doped crystal.[15] The value along the backbone is somewhat smaller in an isolated chain, 0.093, so a value around 0.1 seems suitable to estimate both μ and N_p. We emphasize that even if the simple Drude model can describe very well the spectroscopic optical data values, the interpretation of the model parameters cannot be rigorous but phenomenological. That is, the variations in model parameters in a series of samples are meaningful to monitor relative changes in the corresponding magnitudes such as ρ, μ, and N_p, but their absolute values are less significant.

Figure 1a shows the complex refractive index components $n + ik = \sqrt{\varepsilon}$ obtained for several films studied in this work. Since all the fit functions are parametrized using eq 1, we display values extrapolated to lower energy which are relevant for the discussion when the best fit results for both isotropic and anisotropic models are compared. Regarding the anisotropic components, PEDOT:PSS films display positive birefringence, that is, the extraordinary (out-of-plane) refractive index is larger than the ordinary (in-plane) one. The spectral behaviors agree with the in-plane arrangement of PEDOT backbones and obvious conductive behavior of the corresponding component compared to the out-of-plane nonmetallic character. As can be expected from the measurement configuration, the general spectral behavior of the isotropic solution is similar to that of the anisotropic in-plane component.[16] However, its value is not in between both anisotropic components but it is lower, which seems counterintuitive but is a consequence of the positive birefringent film optics, as in other layered crystals.[17] It is worth noticing that although the fit in the thick bulk-like drop-cast film data is improved with the anisotropic model (MSE reduced by a factor 1.5, see Figure S1), the improvement is most evident in the thinner films when optical interferences appear, from the ∼1 μm thick film (shown in Figure 1b, see also Figure S2) down to device-relevant thicknesses of around 60 nm, which cannot even be properly fitted using eq 1 and an isotropic optical model (see Figure S3) even if the anisotropy is comparatively smaller than in the drop-cast (see Figure S4). In these latter cases, the MSEs are reduced almost 1 order of magnitude. The discrepancies using isotropic models are visually quite clear at angles of incidence around the Brewster angle, which for these films is close to 55 degrees. The Drude parameters determined using the isotropic model are unreliable, in particular both ε_∞ and Γ_p are underestimated, whereas E_p is overestimated (see Figure S4). However, since these parameters are phenomenological, following their variations in series of samples using the isotropic approximation can also be useful to establish trends. A more important drawback is that the fitted film thickness also becomes inaccurate for the isotropic approximation in the thinner films, as verified by complementary profilometer measurements.

In order to reproduce the measured spectral dispersions using eq 1, we need to include up to three CP terms: A rather weak structure is often detected close to 1.5 eV which corresponds to the polaron absorption, a prominent peak observed around 5.3 eV, which has been attributed to the PSS component, and a higher energy broad peak that represents the contribution of higher lying absorptions in a phenomenological way. This third component is actually added for convenience, as it helps to correctly match the experimental background of the spectra. However, this last term alters the proper value of ε_∞. Therefore, to obtain reliable Drude parameters from the fits using eq 1, it is convenient to consider just the two first terms and restrict the spectral range for fitting to the lower energy portion of the spectra, as recommended by Humlicek et al.[14] A convenient cutoff energy in our case is 3 eV, where $k \approx 0$. Since for PEDOT:PSS a weak polaron contribution may be present in the fitted range, in this work, we keep three terms, including one possible CP to represent the polaron, to obtain accurate parameters for use in eq 2. The relevant Drude parameters obtained for films plotted in Figure 1 are listed in Table 1 together with other pertinent results.

In summary, the analysis of ellipsometric data provides both values of film thickness and optical functions whose spectral characteristics can be quantitatively related to the metallic behavior of the PEDOT:PSS films, in particular, revealing information about effective doping and electrical parameters. All these magnitudes are seen to depend not only on the specific formulation (or PEDOT to PSS ratio) but also on structural variations that occur during deposition or post treatment.

2.2.2. Interpretation of Raman Spectra. Raman spectroscopy is a well-established optical method to obtain structural fingerprints based on the measured vibrational signatures of the samples. In particular, it has been extensively applied to PEDOT:PSS based on experimental knowledge and the vibrational modes calculations performed by Garreau et al.,[18] which help to assign the origin of each mode in PEDOT and deliver valuable insights into the structural transformations of PEDOT upon doping. Despite all this knowledge, controversial

https://doi.org/10.1021/acsomega.2c05945
ACS Omega 2022, 7, 39429−39436

Table 1. Parameters Determined from Ellipsometry and Raman Spectra for Selected Samples Studied in This Work[a]

deposition	Δn (2.5 eV)	ε_∞	E_p(eV)	Γ_p(eV)	ω (cm^{-1})	$\Delta\omega$ (cm^{-1})
PEDOT:PSS Sigma-Aldrich 483095 (1:1.6 ratio by weight)						
BC	0.20	2.68	1.28	0.51	1422	41
DC	0.36	2.78	1.48	0.70	1422	41
DC & DMSO	0.15	2.59	1.67	0.82	1427	41
PEDOT:PSS Heraeus Clevios AI4083 (1:6 ratio by weight)						
BC	0.01	2.52	1.27	0.67	1437	44
BC	0.12	2.58	1.03	0.72	1432	42
DC	0.12	2.56	1.01	0.74	1431	43
DC & DMSO	0.04	2.68	1.10	0.74	1429	39

[a]The deposition methods are abbreviated as BC (blade coating) and DC (drop casting). The birefringence $\Delta n = n_e - n_o$ is given at an energy of 2.5 eV as an indication of the optical anisotropy of each film. The Drude parameters correspond to the ordinary component.

statements are found in this abundant literature when partial evidence coming just from Raman spectra are considered. In this context, it is useful to discuss both vibrational and optical spectra together because insights gained from both methods are complementary, allowing us to clarify the interpretation of Raman spectra.

It is well-known that the Raman spectra of PEDOT:PSS show some dependence with the laser excitation wavelength with usual lasers in the near-infrared and visible range. In particular, the position of the Raman bands which are associated with the π-bonding system exhibit small shifts with different wavelength excitation due to preferential resonant enhancement of specific segments of the polymer. Longer wavelengths selectively enhance the segments with longer effective conjugation lengths.[18,19] However, the main interpretation of the spectra is common to all of them and comparison between samples is possible if spectra are measured with the same excitation. In this work, we choose to work with λ = 785 nm (1.58 eV)s because it has a large resonant effect on the segments of the conjugated thiophene backbone that contribute to the electrical conductivity. This is convenient for correlation with the ellipsometric spectra as well as to obtain reasonably intense signals from very thin films, since we must use low laser powers to prevent heating and degradation of the polymer. In addition, degradation is further reduced by using a less energetic laser in the near-infrared.

A typical Raman spectrum is shown in Figure 2. In the fit, each Raman band is initially represented by a pseudo-Voigt function because some bands are better represented by Gaussian and others by Lorentzian lineshapes; once established, these plain lineshapes are chosen. In general, we find that sharper modes are Lorentzian and broader ones are Gaussian. Some bands are obviously asymmetric and are fitted by split profiles. The most intense band near 1422 cm^{-1} is always well reproduced by a symmetric profile with mixed pseudo-Voigt line shape. The modes that are sensitive to changes in conjugation length are those above 1200 cm^{-1}, as is clear from Figure 3. Among them, the most intense band shows the largest variation upon doping, spanning about 25 cm^{-1} total shift in the PEDOT:PSS complex.[20] This large variation may be an apparent effect since the band possibly contains two components.[20,21] However, these components do not always appear resolved and experimentally it is practical to just fit one average peak. The origin of these two assumed components is the benzoid-quinoid tautomerism of PEDOT chains, in which the higher-frequency component would arise from the benzoid structure and the lower-frequency one from the quinoid, agreeing with a longer conjugation length in the latter. This is an idealization because a continuous distribution of molecular conformations is the most probable scenario. Experimentally, the shift upon doping is to the blue, leading to a contradiction with the ground state of PEDOT being aromatic.[22] In addition, calculations support the change to quinoid conformation by doping.[23] Therefore, other mechanisms must counterbalance and be more effective in shortening the conjugation length by increasing doping and the observed Raman shifts cannot be simply interpreted in terms of quinoid to benzoid transformation as frequently done. One possibility could be some twisting of the thiophene backbone,[24] even if PEDOT is considered to be essentially planar. In addition,

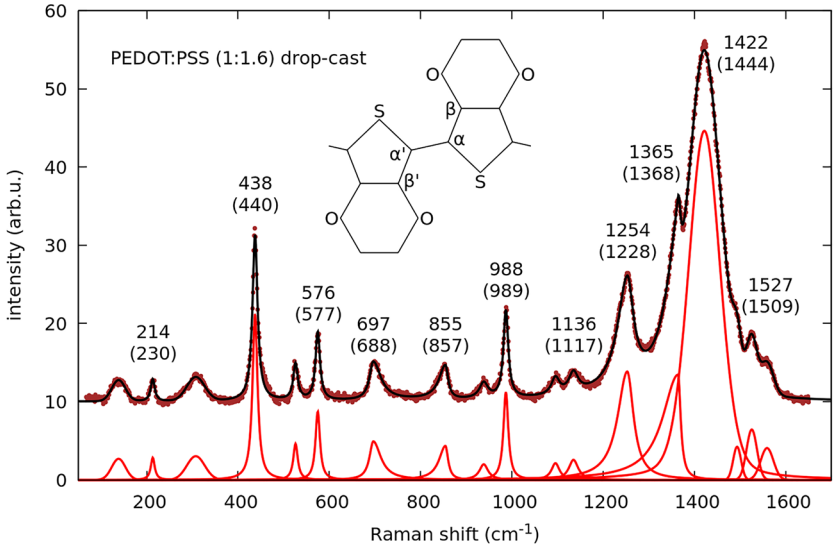

Figure 2. Raman spectrum measured in a dropcast Sigma-Aldrich 483095 PEDOT:PSS film. The fitted components are shown and the obtained Raman shifts are compared to calculated frequencies for PEDOT, given in parentheses according to values tabulated in ref 18.

https://doi.org/10.1021/acsomega.2c05945
ACS Omega 2022, 7, 39429−39436

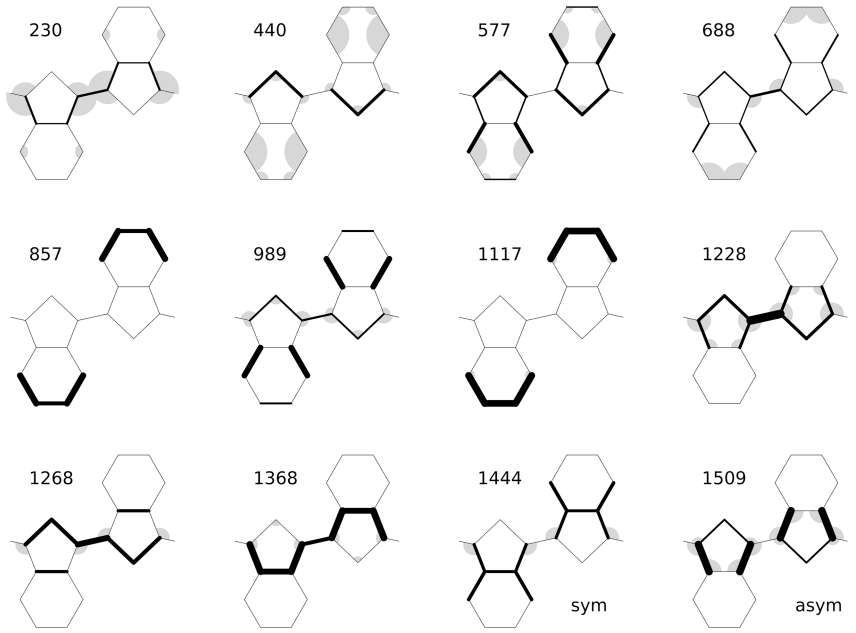

Figure 3. Graphical representation of the main modes of PEDOT according to calculated values tabulated in ref 18. Main bond contributions are represented here by thicker lines, and angles are also proportionally drawn to their variations.

both intrachain linearity and interchain packing enhance conjugation.

Enhanced linearity is associated with the quinoid conformation. On the other side, enhanced planarity results from PEDOT agglomeration and alignment into large domains. This second mechanism, which is more related to film morphology, could be the dominant one in a real film with phase separation. Another relevant parameter is the line width of the main Raman band, which arises from the distribution of conjugation lengths. A narrower band implies more homogeneous distribution of conjugated domains, which usually seems to appear for films with red-shifted Raman, although in principle, the average position and the line width must not necessarily be correlated.

3. RESULTS AND DISCUSSION

3.1. Spectroscopic Results and Discussion. As is the case with the electrical conductivity, the measured optical functions represent the response from the combined PEDOT:PSS medium. In particular, observed anisotropies are the result of morphological characteristics of the conducting PEDOT-rich particles embedded in the rather isolating and isotropic PSS-rich host. Hence, PSS richer films are less anisotropic and display higher electrical resistivity, also according to eq 2. In contrast, Raman scattering is mainly sensitive to PEDOT vibrations; in our experimental conditions, we do not detect any PSS vibrations. However, the results of both optical techniques depend on the general film morphological traits. A systematic investigation of both Raman and optical functions including anisotropy is thus helpful to establish the link between optical and structural properties using noninvasive measurements. In the following, we consider the results from different formulations and morphologies to investigate this link.

3.1.1. Dependence with PSS Content. The two investigated formulations differ mainly in the ratio of PEDOT to PSS. Despite the notable difference of proportions 1:1.6 vs 1:6, in both cases, PSS is present in excess in the PEDOT:PSS polyelectrolyte complex and the oxidation level (doping) of PEDOT can be similarly high. The maximum attainable is around 33% ionized sites, equivalent to one positive charge every three monomer units. As already mentioned, the films consist of PEDOT:PSS grains embedded in an amorphous PSS matrix. The optical properties of the films correspond to this composed medium, in particular, the Drude model parameters of eq 1 reflect the composite behavior, whereas the critical points are characteristic optical transitions more localized in the components. Note that the weak polaronic transition is localized in PEDOT and its absence or weakness qualitatively indicates the high doping level in all studied films. When this band is present, its fitted amplitude correlates with the polaron concentration,[2] which can be compared with the Raman shift evolution. The largest difference in the two studied formulations being the PSS content, is mostly reflected in the Drude parameters. In particular, the plasma energy gives an indication of the overall PSS content. Regarding the optical anisotropy, we already mentioned that it is larger for the lower PSS content Sigma-Aldrich 483095 films but we find that films of Clevios AI4083 are still anisotropic, especially if dropcast.[16] In both formulations, the anisotropy in blade coated films is comparatively smaller due to faster drying which leads to a morphology with smaller phase separation,[12] implying smaller aggregation of PEDOT:PSS grains. Figure 4 shows the complex refractive index components for films of Clevios AI4083 showing different anisotropy. The Raman spectra of the same films show up to 6 cm^{-1} difference in position of the main peak, which is a quite large dispersion compared to 9 cm^{-1} difference in position between the drop-cast films of the two formulations. It seems clear that the usual identification of main Raman peak position, or in other words conjugation length, solely determined by doping of the PEDOT chain is not valid. Interestingly, the Raman results for films of the same formulation displayed in Figure 4 suggest that the different anisotropy is related to different Raman shift (see Table 1). Unfortunately, anisotropy is also related to the PSS content because the PSS matrix is rather isotropic. However, in

https://doi.org/10.1021/acsomega.2c05945
ACS Omega 2022, 7, 39429−39436

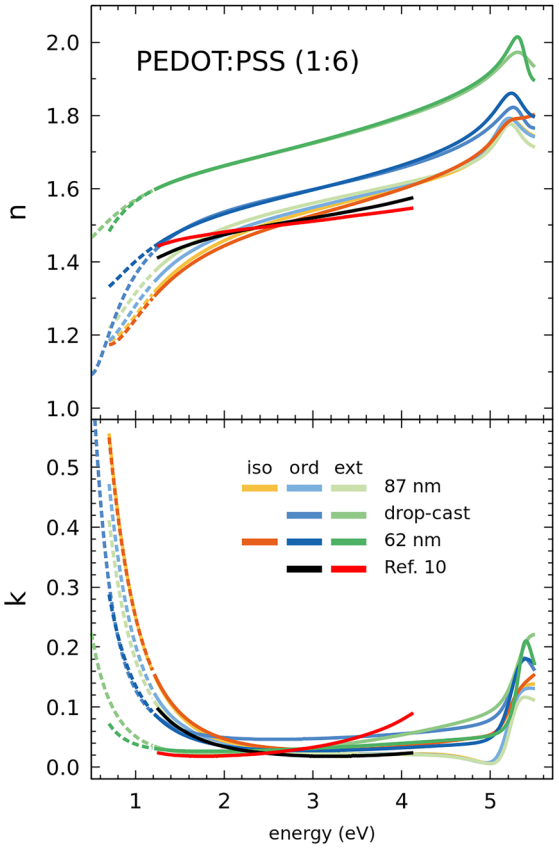

Figure 4. Complex refractive index components for different films of Heraeus Clevios AI4083 PEDOT:PSS. One of the blade coated films, the 87 nm thick one, is almost isotropic, like that from ref 10 plotted for comparison. Results obtained here using both isotropic and anisotropic models for both blade-coated films are shown.

comparable films, increasing anisotropy gives decreasing Raman shift, pointing to an important influence of interchain packing in aggregated grains within the film as mechanism to enhance conjugation length. The broadening is not clearly reduced, suggesting that the dispersion in conjugated lengths changes very little even if the average is enhanced.

3.1.2. Effect of DMSO Addition. The role of morphology regarding the Raman spectra can be further clarified by correlating them with the optical properties of films modified by DMSO addition. The effects of DMSO are most clearly appreciated in drop cast films in which the drying time is longer and changes can develop to a greater extent. Besides, the changes induced by DMSO are also clearer in lower PSS content films, which in our case is the Sigma-Aldrich 483095 formulation. In all cases the measurements were done far from the film border where PSS segregation is noticeable. Relevant resulting parameters for all samples selected in this study are listed in Table 1.

In all cases, DMSO addition tends to reduce the optical anisotropy (see Figures S5−S8). This reduction may be due to smaller PEDOT:PSS grains in the PSS matrix resulting in a lower chain aggregation and/or a lower overall correlation of in-plane order among the grains. At the same time, the optical spectra (Figures S6 and S8) display more clear polaron bands, consistent with the literature,[25] indicating dedoping of the PEDOT:PSS regions. Both facts support the explanation that the higher electrical conductivity is mainly related to a change in phase separation structure that leads to improved connectivity of the PEDOT:PSS regions in the film.[26]

Figure 5 shows the main Raman band for the four drop cast films. The shifts in this band give an indication of the local changes in the PEDOT:PSS grains. Although ellipsometry proves that there is dedoping in both cases, the change in position for every formulation is different. Clearly, the Raman shift is not correlated with the overall PSS content in the film in contradiction with the accepted link between the frequency position of this band and the level of doping, and in particular the large blue shift for the lower PSS containing film suggests that morphology change plays the main role in the shift, which in this case indicates a decrease in conjugation length. In general, taking into account the correlation between the results of both spectroscopies, the position of the main Raman band seems to result from at least two contributions with opposite sign: a red shift generally attributed to dedoping[20,21] and a blue

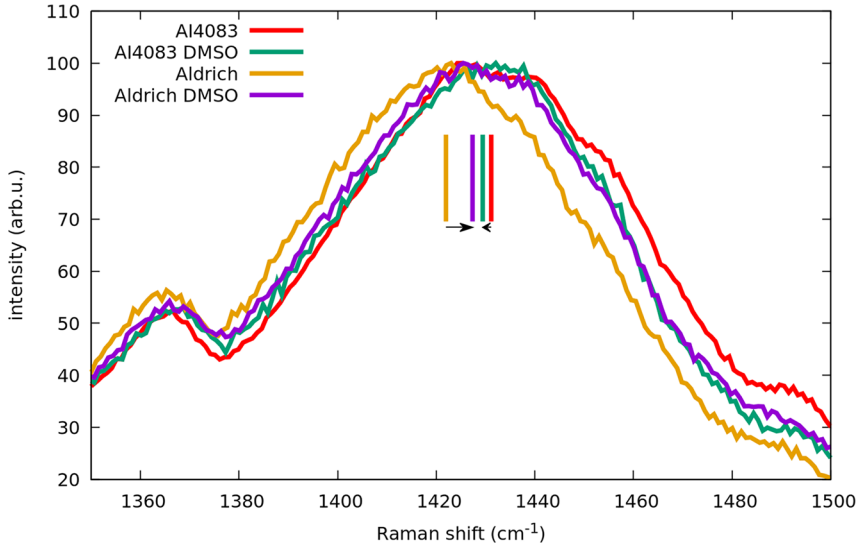

Figure 5. This figure highlights the importance of morphology in the average conjugation length. Dedoping can lead either to red or blue shift of the main Raman band depending on the actual phase separation in the films.

https://doi.org/10.1021/acsomega.2c05945
ACS Omega 2022, 7, 39429−39436

shift that is likely due to a reduction of the grain size, consistent with the measured smaller optical anisotropy. It makes sense that in our experiments the former predominates in the higher PSS content film, where the grains are already small without DMSO, and the latter in the lower PSS content film that has larger aggregates without DMSO, which allow for an increased dispersion of the aggregated domains upon DMSO addition, consistent with recent studies.[26]

CONCLUSIONS

Both spectroscopic ellipsometry and Raman scattering are noninvasive and versatile methods able to probe different structural traits related to the optoelectronic properties of PEDOT:PSS films. The combined study using these optical spectroscopies provides detailed insights into diverse significant aspects of this complex material. The main optical informations extracted from ellipsometry are the optical constants of the composite medium including anisotropic behavior, as well as their spectral characteristics related to average doping and optical conductivity. In addition, interband transitions are signatures of more local properties, in particular the appearance of a weak polaron band is related to the doping state of the PEDOT:PSS domains. On the other hand, the main information obtained from the position of the main Raman band is associated with the conjugation length for PEDOT in the same domains. Previous literature suggested that conjugation length depends only from the chain conformation given by the doping state, roughly related to the PSS content. In this work, we find that the film's phase separation nanomorphology gives a likewise important contribution to the Raman shift. Since the morphology, more specifically the alignment of the fibrils in the PEDOT:PSS domains, is connected to the optical anisotropy, there is a correlation between anisotropy and Raman shift in films with the same PSS content, so that higher anisotropy is found together with a red-shifted Raman band, implying a longer conjugation length.

Films obtained with DMSO addition tend to be less anisotropic. This may seem surprising but is consistent with the morphology change induced by this additive.[26] The segregation of PSS caused by DMSO gives as a result some dedoping and improved alignment of the fibrils in the PEDOT:PSS domains, but it also tends to cause misaligned and smaller aggregated grains that as a result become closer to one another. Hence, even if the conjugation length in a grain may be reduced, their closer proximity can lead to improved optical and electrical conductivity. This effect is largest in the low PSS content formulation we have studied, and is relatively small in the high PSS content formulation, where the phase separation of the pristine films is already quite small.

Finally, we must emphasize that it is very difficult to generalize trends that depend on a complex interplay of different parameters. In fact, not only PSS contents and the different solvent/additives can give rise to films with different properties. Different deposition methods and different conditions can also result in different morphologies. Therefore, the availability of advanced optical characterization procedures as outlined in this study are expected to be very useful in understanding and optimizing PEDOT:PSS films for optical and thermoelectric applications.

ASSOCIATED CONTENT

Supporting Information

The Supporting Information is available free of charge at https://pubs.acs.org/doi/10.1021/acsomega.2c05945.

Information about materials, experimental setups, and complementary ellipsometry spectra analysis and resulting optical functions (PDF)

AUTHOR INFORMATION

Corresponding Author

Maria Isabel Alonso − *Institut de Ciència de Materials de Barcelona, ICMAB-CSIC, Campus UAB, Bellaterra 08193, Spain;* orcid.org/0000-0001-7669-5871; Email: isabel@icmab.es

Authors

Minghua Kong − *Institut de Ciència de Materials de Barcelona, ICMAB-CSIC, Campus UAB, Bellaterra 08193, Spain*

Miquel Garriga − *Institut de Ciència de Materials de Barcelona, ICMAB-CSIC, Campus UAB, Bellaterra 08193, Spain*

Juan Sebastián Reparaz − *Institut de Ciència de Materials de Barcelona, ICMAB-CSIC, Campus UAB, Bellaterra 08193, Spain*

Complete contact information is available at: https://pubs.acs.org/10.1021/acsomega.2c05945

Author Contributions

The manuscript was written through contributions of all authors. All authors have given approval to the final version of the manuscript.

Notes

The authors declare no competing financial interest.

ACKNOWLEDGMENTS

The authors acknowledge funding from the Spanish Ministerio de Ciencia e Innovación (MICINN) through grants PID2019-106860GB-I00 and PID2020-119777GB-I00 and the Spanish Severo Ochoa Centre of Excellence program CEX2019-000917-S, as well as AGAUR, Generalitat de Catalunya, grant 2017-SGR-00488. M.K. is grateful to the UAB PhD program in Materials Science in which she is enrolled and the China Scholarship Council for funding (CSC 201809370071). We thank Agustín Mihi and Mariano Campoy-Quiles for their constant support and ideas.

ABBREVIATIONS

PEDOT, poly(3,4-ethylenedioxythiophene); PSS, poly(styrenesulfonate); UV, ultraviolet; DMSO, dimethyl sulfoxide

REFERENCES

(1) Elschner, A., Kirchmeyer, S., Lövenich, W., Merker Udo, R. K.*PEDOT Principles and Applications of an Intrinsically Conducting Polymer*; CRC Press: Boca Raton, FL, 2011.

(2) Kim, N.; Petsagkourakis, I.; Chen, S.; Berggren, M.; Crispin, X.; Jonsson, M. P.; Zozoulenko, I. Electric Transport Properties in PEDOT Thin Films. *Conjug. Polym.* **2019**, 45−128.

(3) Pettersson, L. A. A.; Ghosh, S.; Inganäs, O. Optical Anisotropy in Thin Films of Poly(3,4-Ethylenedioxythiophene)-Poly(4-Styrenesulfonate). *Org. Electron.* **2002**, *3* (3−4), 143−148.

(4) Syrovy, T.; Janicek, P.; Mistrik, J.; Palka, K.; Hawlova, P.; Kubac, L.; Gunde, M. K. Optical, Electrical and Morphological Study of PEDOT: PSS Single Layers Spiral-Bar Coated with Various Secondary Doping Solvents. *Synth. Met.* **2017**, *227*, 139−147.
(5) Laskarakis, A.; Karagkiozaki, V.; Georgiou, D.; Gravalidis, C.; Logothetidis, S. Insights on the Optical Properties of Poly(3,4-Ethylenedioxythiophene): Poly(Styrenesulfonate) Formulations by Optical Metrology. *Materials (Basel).* **2017**, *10* (8), 959.
(6) Pettersson, L. A. A.; Roman, L. S.; Inganäs, O. Modeling Photocurrent Action Spectra of Photovoltaic Devices Based on Organic Thin Films. *J. Appl. Phys.* **1999**, *86* (1), 487.
(7) Isoniemi, T.; Tuukkanen, S.; Cameron, D. C.; Simonen, J.; Toppari, J. J. Measuring Optical Anisotropy in Poly(3,4-Ethylene Dioxythiophene):Poly(Styrene Sulfonate) Films with Added Graphene. *Org. Electron.* **2015**, *25*, 317−323.
(8) Liu, Q.; Imamura, T.; Hiate, T.; Khatri, I.; Tang, Z.; Ishikawa, R.; Ueno, K.; Shirai, H. Optical Anisotropy in Solvent-Modified Poly(3,4-Ethylenedioxythiophene): Poly(Styrenesulfonic Acid) and Its Effect on the Photovoltaic Performance of Crystalline Silicon/Organic Heterojunction Solar Cells. *Appl. Phys. Lett.* **2013**, *102* (24), 243902.
(9) Lin, Y.; Zhao, Y.; Xin, Q.; Jiang, C.; Song, A. Electrical Control of the Optical Dielectric Properties of PEDOT:PSS Thin Films. *Opt. Mater. (Amst).* **2020**, *108*, 110435.
(10) Mauger, S. A.; Moulé, A. J. Characterization of New Transparent Organic Electrode Materials. *Org. Electron.* **2011**, *12*, 1948−1956.
(11) Nardes, A. M.; Kemerink, M.; Janssen, R. A. J.; Bastiaansen, J. A. M.; Kiggen, N. M. M.; Langeveld, B. M. W.; Van Breemen, A. J. J. M.; De Kok, M. M. Microscopic Understanding of the Anisotropic Conductivity of PEDOT:PSS Thin Films. *Adv. Mater.* **2007**, *19* (9), 1196−1200.
(12) Ouyang, L.; Musumeci, C.; Jafari, M. J.; Ederth, T.; Inganäs, O. Imaging the Phase Separation between PEDOT and Polyelectrolytes during Processing of Highly Conductive PEDOT:PSS Films. *ACS Appl. Mater. Interfaces* **2015**, *7* (35), 19764−19773.
(13) *Spectroscopic Ellipsometry for Photovoltaics*; Fujiwara, H., Collins, R. W., Eds.; Springer Series in Optical Sciences; Springer, 2018; Vol. *212*.
(14) Humlíček, J.; Nebojsa, A.; Hora, J.; Stráský, M.; Spousta, J.; Šikola, T. Ellipsometry and Transport Studies of Thin-Film Metal Nitrides. *Thin Solid Films* **1998**, *332* (1−2), 25−29.
(15) Kim, E. G.; Brédas, J. L. Electronic Evolution of Poly(3,4-Ethylenedioxythiophene) (PEDOT): From the Isolated Chain to the Pristine and Heavily Doped Crystals. *J. Am. Chem. Soc.* **2008**, *130* (50), 16880−16889.
(16) Campoy-Quiles, M.; Alonso, M. I.; Bradley, D. D. C.; Richter, L. J. Advanced Ellipsometric Characterization of Conjugated Polymer Films. *Adv. Funct. Mater.* **2014**, *24* (15), 2116−2134.
(17) Alonso, M. I.; Tortosa, S.; Garriga, M.; Piñol, S. Ellipsometric Measurement of the Dielectric Tensor of Nd 2 - x Ce x CuO 4 - *δ*. *Phys. Rev. B* **1997**, *55* (5), 3216−3221.
(18) Garreau, S.; Louarn, G.; Buisson, J. P.; Froyer, G.; Lefrant, S. In Situ Spectroelectrochemical Raman Studies of Poly(3,4-Ethylenedioxythiophene) (PEDT). *Macromolecules* **1999**, *32* (20), 6807−6812.
(19) Stavytska-Barba, M.; Kelley, A. M. Surface Enhanced Raman Study of the Interaction of PEDOT:PSS with Silver and Gold Nanoparticles. *J. Phys. Chem. C* **2010**, *114*, 6822−6830.
(20) Chiu, W. W.; Travaš-Sejdić, J.; Cooney, R. P.; Bowmaker, G. A. Studies of Dopant Effects in Poly(3,4-Ethylenedioxythiophene) Using Raman Spectroscopy. *J. Raman Spectrosc.* **2006**, *37* (12), 1354−1361.
(21) Nešpůrek, S.; Kuberský, P.; Polanský, R.; Trchová, M.; Šebera, J.; Sychrovský, V. Raman Spectroscopy and DFT Calculations of PEDOT:PSS in a Dipolar Field. *Phys. Chem. Chem. Phys.* **2021**, *24* (1), 541−550.
(22) Dkhissi, A.; Louwet, F.; Groenendaal, L.; Beljonne, D.; Lazzaroni, R.; Brédas, J. L. Theoretical Investigation of the Nature of the Ground State in the Low-Bandgap Conjugated Polymer, Poly(3,4-Ethylenedioxythiophene). *Chem. Phys. Lett.* **2002**, *359* (5−6), 466−472.
(23) Lenz, A.; Kariis, H.; Pohl, A.; Persson, P.; Ojamäe, L. The Electronic Structure and Reflectivity of PEDOT:PSS from Density Functional Theory. *Chem. Phys.* **2011**, *384* (1−3), 44−51.
(24) Garreau, S.; Leclerc, M.; Errien, N.; Louarn, G. Planar-to-Nonplanar Conformational Transition in Thermochromic Polythiophenes: A Spectroscopic Study. *Macromolecules* **2003**, *36* (3), 692−697.
(25) Gasiorowski, J.; Menon, R.; Hingerl, K.; Dachev, M.; Sariciftci, N. S. Surface Morphology, Optical Properties and Conductivity Changes of Poly(3,4-Ethylenedioxythiophene):Poly-(Styrenesulfonate) by Using Additives. *Thin Solid Films* **2013**, *536*, 211−215.
(26) Heroux, L.; Moncada, J.; Dadmun, M. Controlling the Morphology of PEDOT:PSS Blend Films with Pre-Deposition Solution Composition and Deposition Technique. *ACS Appl. Polym. Mater.* **2022**, *4* (1), 36−43.

https://doi.org/10.1021/acsomega.2c05945
ACS Omega 2022, 7, 39429−39436